International Journal of GEOMATE, May 2023, Vol. 24, Issue 105, pp.50-57
ISSN: 2186-2982 (P), 2186-2990 (O), Japan, DOI: https://doi.org/10.21660/2023.105.g12217
Geotechnique, Construction Materials and Environment

MODEL TESTS ON RESPONSE OF CONCRETE BLOCK ON SEABED SUBJECTED TO UPWARD SEEPAGE FLOW

*Tatsuya Matsuda[1], Kinya Miura[1], Naoto Naito[1] and Yuki Ando[1]

[1]Department of Architecture and Civil Engineering, Toyohashi University of Technology, Japan

*Corresponding Author, Received:14 April 2022, Revised: 24 Feb. 2023, Accepted: 12 March 2023

ABSTRACT: Under stormy weather conditions, offshore structures have been severely damaged by heavy sea wave loading. Many researchers have conducted investigations on damaged structures and revealed that the damage to the structures is emphasized by the disintegration of the seabed caused by sea wave loading on the seabed. The previous study by authors conducted model sea-wave loading tests on sand ground and revealed that the disintegration of the seabed and associated scouring were caused by the upward seepage flow as a response to sea-wave loading, which reduced the effective stress in the seabed. Breakwaters consisting of concrete blocks have been monitored for years, and it has been reported that they sink every year by a fraction of a meter in accordance with stormy wave conditions. This study conducted a series of model tests on a block equipped with a three-axial accelerometer to detect its attitude when rested on a seabed with generated upward seepage flow. The sinking behavior of the block in the seabed during the gradual increase in the hydraulic gradient of seepage flow was carefully observed to clarify the fundamental mechanism of the sinking of the block. Consequently, this study found the critical condition of the hydraulic gradient under which the sinking of the block is initiated is independent of the density of the seabed material. In the scheme of model tests, the applicability of the three-axis accelerometer for the detection of the block, even under the critical hydraulic gradient attained, was demonstrated.

Keywords: Model Test, Upward Seepage flow, Seabed, Concrete Block, Bearing Capacity

1. INTRODUCTION

Under stormy weather conditions, offshore structures have been severely damaged by heavy sea wave loading. Breakwaters consisting of concrete blocks have been monitored for years, and it has been reported that they sink every year by a fraction of a meter in accordance with stormy wave conditions. Many researchers have conducted investigations on damaged structures and revealed that the damage to the structures is emphasized by the disintegration of the seabed caused by sea wave loading on the seabed [1].

The fluctuation of effective stress in the seabed is caused by the upward and downward seepage flows during cyclic sea wave loading. This mechanism has been investigated both theoretically and experimentally. For example, Yamamoto et al. (1978) [2] showed an analytical solution for the effective stress response in seabed-induced ocean waves. Miura et al. (2004) [3] qualitatively examined the relationship between the effective stress response of seabed ground and sediment transport in response to progressive, steady, and irregular waves. Zen and Yamazaki (1990) [4] clarified the mechanism of wave-induced liquefaction and densification in permeable seabed using model tests. They also showed that heavy structures may submerge into the seabed, and lightweight structures may rise from the seabed.

Baldock and Holme (1998) [5] discussed the effects of seepage on the transport of sediment by waves and currents. The results showed that upward seepage increased wave-induced erosion, whereas downward seepage stabilized the bottom sediments. Matsuda et al. (2019) [6] conducted model sea wave loading tests on sand ground and revealed that the disintegration of the seabed and associated scouring are caused by the upward seepage flow as a response to sea wave loading, which reduces the effective stress in the seabed. The wave response of rectangular blocks on a sandy substrate was also examined. Accelerometers installed on the blocks showed that the blocks on the sandy bottom tended to tilt offshore under the action of waves. However, it is necessary to discuss the response of blocks on a sand bed subjected to wave-induced seepage forces in more detail.

In this study, a series of model tests was conducted to clarify the behavior of a block on the seabed under the action of an upward seepage flow. To clarify the fundamental mechanism of a block settling, the behavior of the block settling into the seabed as the hydrodynamic gradient of the seepage flow gradually increased was carefully observed using sensors for acceleration and displacement. Pertinent discussion on block behavior subjected to seepage failure of ground, settlement phenomena and rate of block are depicted.

2. RESEARCH SIGNIFICANCE

This study clarifies the characteristics of the settlement behavior of blocks with different types and densities of geomaterials. Since previous studies have not shown a clear scale law in the geomaterials used in the model tests, this experiment will provide useful results. The clarification of the mechanism of settlement of the blocks will lead to the proposal of countermeasures. Furthermore, it can provide criteria for evaluating the stability of the blocks in their maintenance.

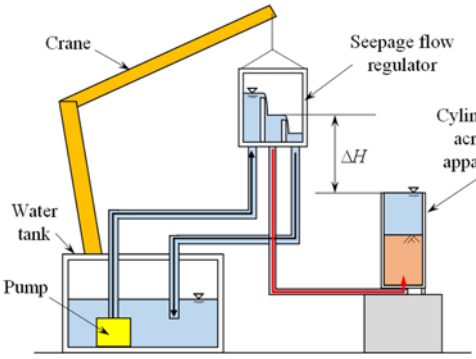

Fig.1 Schematic of model test system

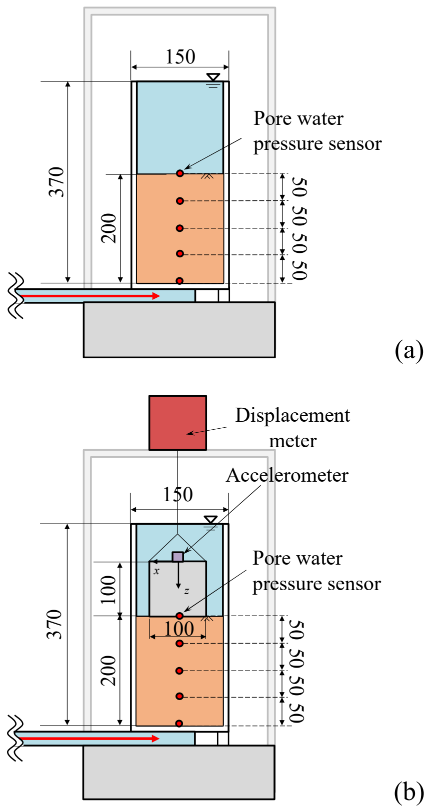

Fig.2 Schematic of model test condition: Case of ground only condition (a) and Case of rectangular block placed on the Ground condition (b)

3. MODEL LOADING TESTS

3.1 Model Test System and Measurement Device

Figs. 1 and 2 shows a schematic of the one-dimensional seepage test device system and schematic of model test conditions. A cylindrical acrylic apparatus with a height of 370 mm and diameter of 150 mm was used in these tests. A drainage valve was installed at the bottom of the apparatus, which was connected to the seepage flow regulator using a pipe. The seepage flow regulator was equipped with a drainage weir such that the water level was maintained at a constant level in the device. The height of the apparatus was adjusted using a crane to change the water level difference (ΔH) between the seepage flow regulator and the cylindrical acrylic apparatus. In all the model tests, a 200 mm thick layer of soil was prepared to achieve a given density. To measure the pore water pressure

Table 1 Physical properties of geomaterials

	Toyoura sand	Silica #8
D_{50} (mm)	0.189	0.109
e_{max}	0.999	1.218
e_{min}	0.632	0.670
G_s	2.668	2.681

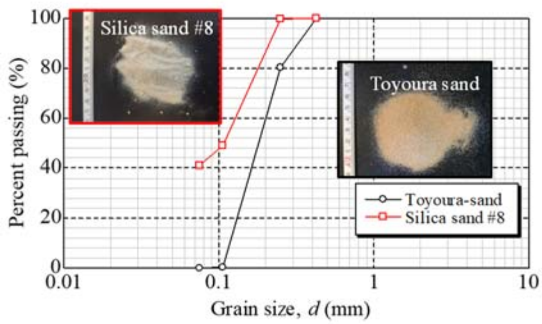

Fig.3 Particle size distribution of geomaterials

Table 2 Model test cases

Case	Geomaterial	Relative density, D_r (%)	Block
Case-T40	Toyoura sand	40	None
Case-T70	Toyoura sand	70	None
Case-S40	Silica sand #8	40	None
Case-S70	Silica sand #8	70	None
Case-T40B	Toyoura sand	40	Exist
Case-T70B	Toyoura sand	70	Exist
Case-S40B	Silica sand #8	40	Exist
Case-S70B	Silica sand #8	70	Exist

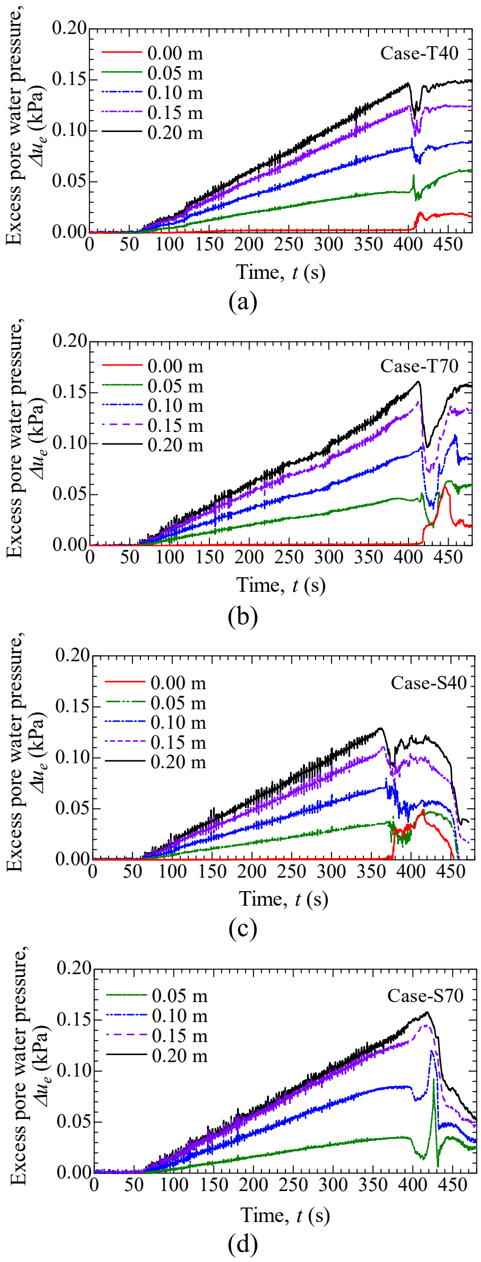

Fig. 4 Time histories of excess pore water pressure in case of soil ground only: Case-T40 (a); Case-T70 (b); Case-S40 (c) and Case-S70 (d).

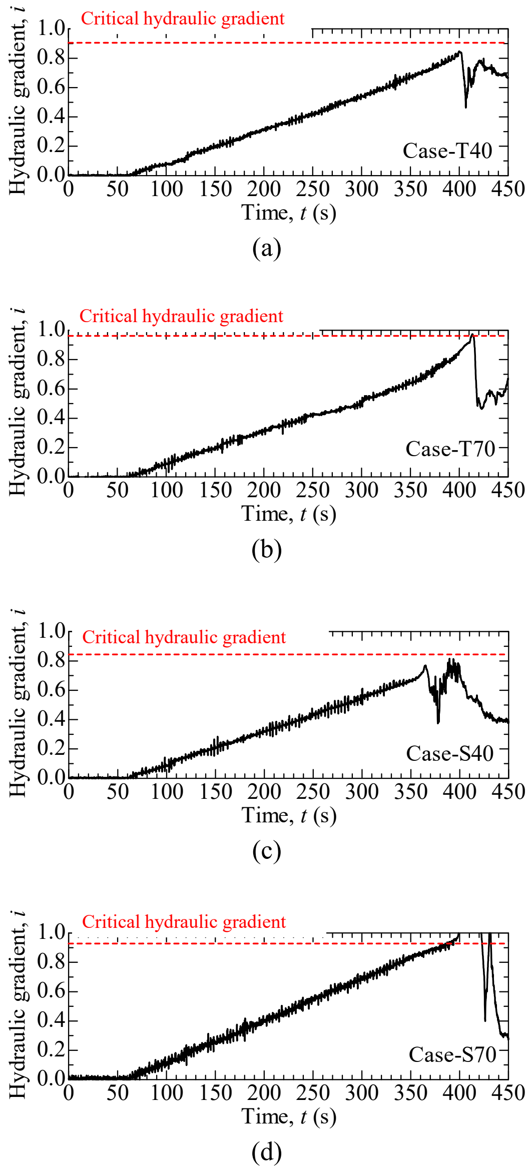

Fig. 5 Time histories of hydraulic gradient in case of soil ground only: Case-T40 (a); Case-T70 (b); Case-S40 (c) and Case-S70 (d).

in the ground, five pore water pressure sensors were installed in the soil at the interior wall of the apparatus at intervals of 50 mm from the bottom of the apparatus. In addition, a three-axis accelerometer and displacement transducer were installed at the center of the top of the block to measure its behavior.

3.2 Model Test Condition

Toyoura sand and silica sand No. 8 (hereinafter referred to as silica sand #8) were used as geomaterials in this test. Table 1 lists the properties of the soil materials and Fig. 3 shows the particle size distribution. The reason for using this geomaterial was due to the application of Dean Number [7]. Dean Number is a dimensionless of fall speed parameter, given as the following equation;

$$\left[w/(H/T)\right]_p = \left[w/(H/T)\right]_m \tag{1}$$

where, w, H, and T are vertical fall speed of a soil particle in the fluid, wave height and wave period, respectively. The subscript of p and m means prototype and model.

The geomaterial in model sediment which is

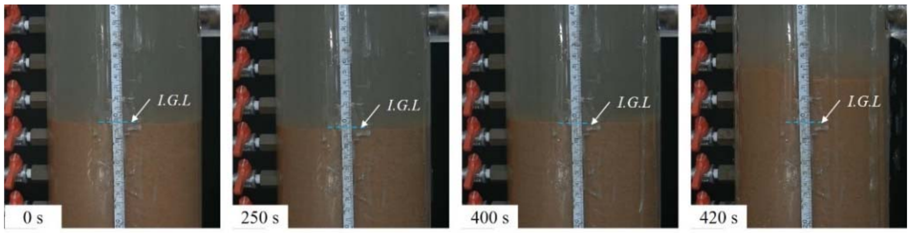

(a)

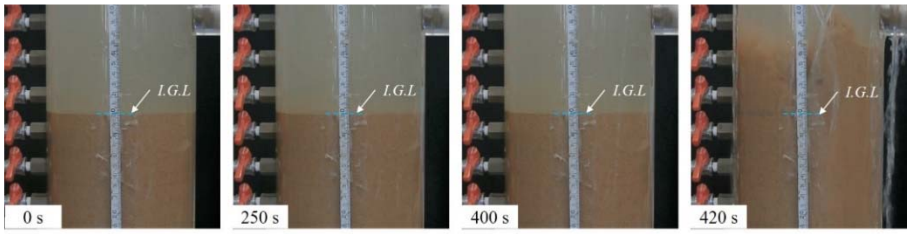

(b)

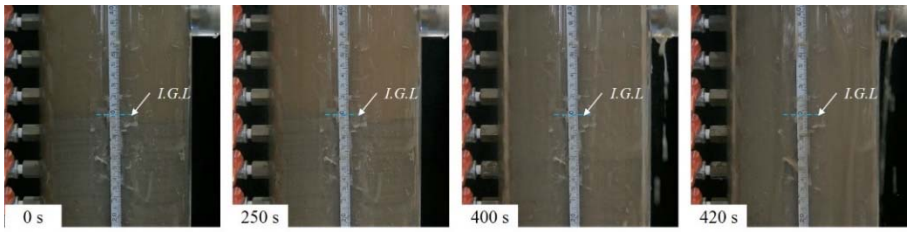

(c)

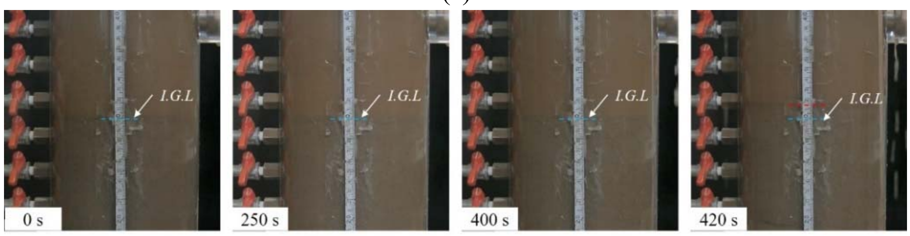

(d)

Fig. 6 Time histories of soil ground change due to upward seepage flow in case of soil ground only: Case-T40 (a); Case-T70 (b); Case-S40 (c) and Case-S70 (d).

applied to the Dean Number is classified as fine sand ($D_{50}|m$ = 0.08 mm) when the prototype is fine sand ($D_{50}|p$ = 0.20 mm). Toyoura sand was used as the material in prototype and silica sand No. 8 was used as the material to which the Dean Number was applied. The model ground was deposited by the underwater dropping method using a specified amount of soil measured to obtain target relative densities of D_r = 40 % and 70 %. Two cases were considered in the tests: a ground-only case without blocks and a case with blocks placed on the ground surface. Table 2 lists the experimental conditions for each case. The concrete block used was a cube with dimensions of 100 × 100 × 100 mm and weight of 2.2 kg.

3.3 External Force Condition

The loading conditions for the seepage force were the same for all the experimental cases. The seepage flow regulator was kept stationary with a zero-water level difference for up to 60 s after the start of the experiment; subsequently, it was raised at a rate of 0.05 mm/s and the seepage force was applied. Thereafter, while maintaining the critical dynamic hydraulic gradient, the seepage force was applied until the ground collapsed in the case of the ground only and until 1200 s in the case with the block.

4. MODEL TEST RESULTS

4.1 Case of Soil Ground Only

This section presents a discussion of the seepage failure of the soil ground in the absence of block. Fig. 4 shows the time history of the excess pore water pressure for each case. The pore water

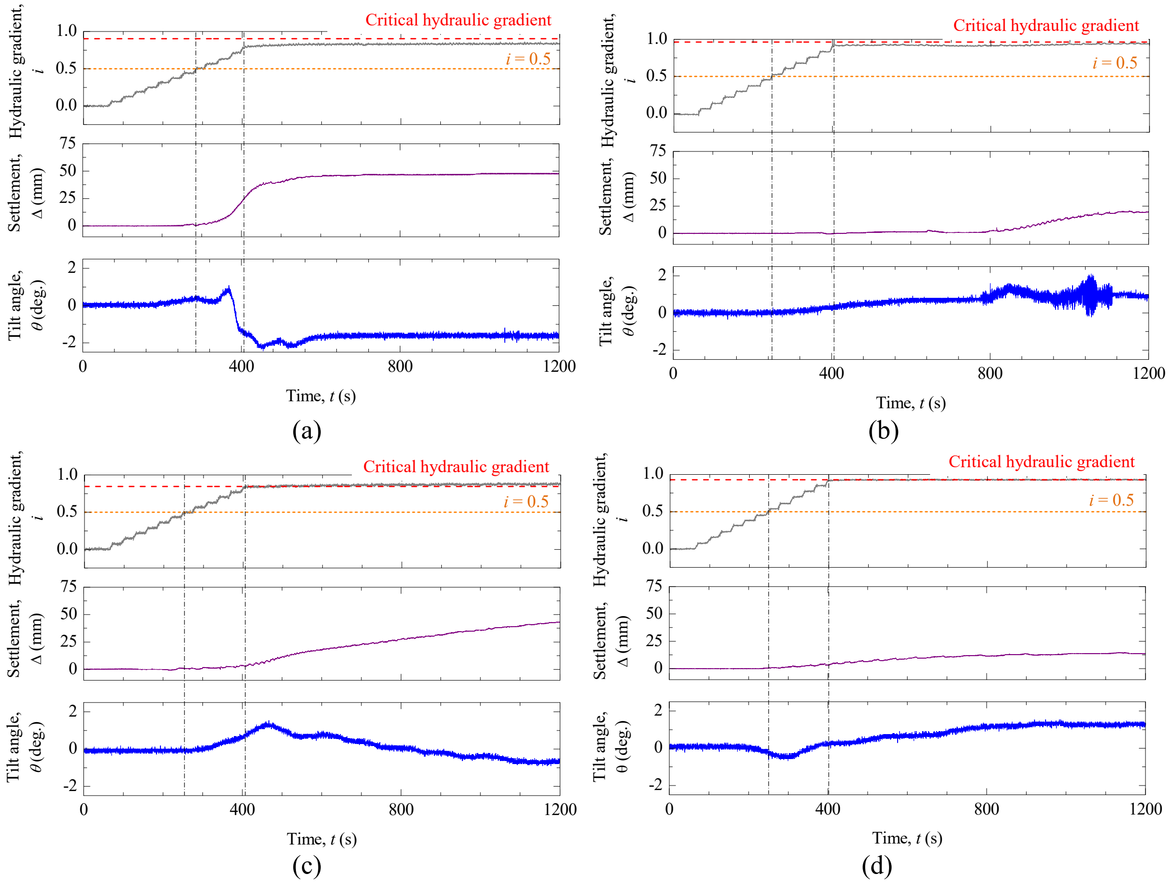

Fig. 7 Time histories of the hydraulic gradient in the ground (top), the amount of settlement of the block (middle), and the tilt angle of a block (low): Case-T40B (a); Case-T70B (b); Case-S40B (c) and Case-S70B (d).

pressure sensor at $z = 0.20$ m, the lowest point of the ground, was lower than the increment of pore water pressure caused by the difference in hydraulic head. This cause was due to the influence of the boundary. The same trend was observed in all the cases. In Case-S70, the pore water pressure at z = 0.00 m from the ground surface could not be measured accurately. Therefore, the following hydrodynamic gradient values were calculated using the measured heights of $z = 0.05$ m and 0.15 m, which had stable values, to consider spatial variations in the ground. Hydraulic gradient i and critical hydraulic gradient i_{cr} were calculated using the following equations:

$$i = \frac{\left(\Delta u_e\big|_{z=0.15} - \Delta u_e\big|_{z=0.05}\right)/\gamma_w}{0.15-0.05} \quad (2)$$

$$i_{cr} = \frac{G_s - 1}{1+e} \quad (3)$$

where Δu_e is the excess pore water pressure, γ_w is the unit weight of water, G_s is the specific gravity weight of the soil particles, and e is the void ratio.

Fig. 5 shows the change in the hydraulic gradient of the ground over time. Generally, the hydraulic gradient did not differ depending on the geomaterials, but differences were observed around the critical hydraulic gradient with the soil density.

For example, in the loose ground with 40 % relative density, the hydraulic gradient changed significantly when it reached approximately 90 % of the critical hydraulic gradient (Figs. 5(a) and (c)). On the other hand, in the case of the middle dense ground with 70 % relative density, the hydraulic gradient changed after the critical hydraulic gradient was reached (Figs. 5(b) and (d)). In both cases, there was no significant difference in the hydraulic gradient depending on the geomaterial, suggesting that seepage failure occurred when the hydraulic gradient value changed significantly.

Fig. 6 shows the ground conditions at the initial condition ($t = 0$ s) in the region where the hydraulic gradient reached 0.5 ($t = 250$ s) and near the critical hydraulic gradient ($t = 400$ and 420 s), respectively. The ground elevation did not change at a hydraulic gradient of 0.5 in each case. However, the location

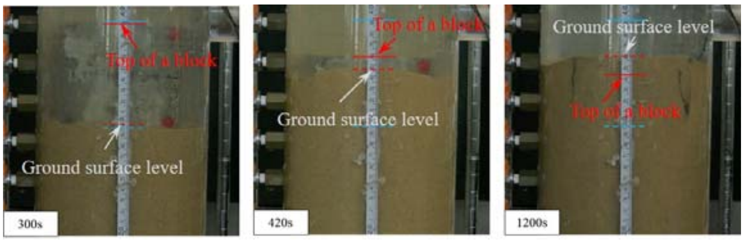

(a)

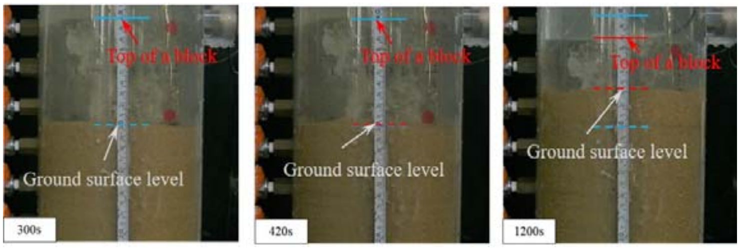

(b)

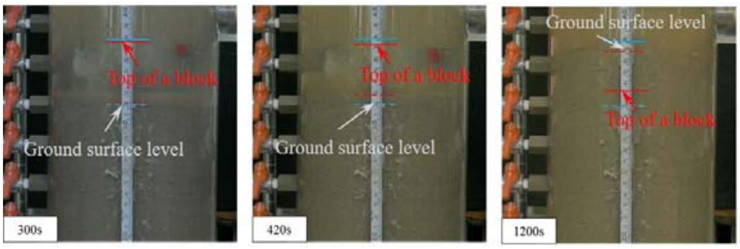

(c)

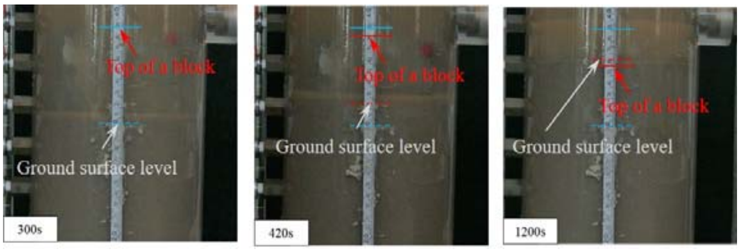

(d)

Fig. 8 Change of ground surface level due to upward seepage flow and a block behavior at 300 s, 420 s and 1,200 s: Case-T40B (a); Case-T70B (b); Case-S40B (c) and Case-S70B (d).

of the ground surface could not be determined because Case-S40 failed at 400 s. In other cases, no change from the initial ground surface was observed. In Cases T40, T70, and S70, the hydraulic gradient changed significantly near the critical hydraulic gradient, and failure occurred along with boiling. This suggests that the deformation of the ground when seepage forces cause seepage failure is not gradual but rather occurs rapidly when the critical hydrodynamic gradient is reached. This is consistent with the experimental results of Yoshimi et al. (1973) [8].

4.2 Case of Block Placed on the Ground

This section investigates the behavior of the ground and blocks when subjected to seepage forces. Fig. 7 shows the time histories of the hydraulic gradient in the ground, the amount of settlement of the block measured by the displacement meter, and the tilt angle of the block from the initial state, which is calculated from the change in the acceleration sensor in each case. The tilt angle of a block θ is calculated as following equation:

$$\theta = \sin^{-1} \frac{a_x}{g} \tag{4}$$

here, a_x and g are the horizontal and gravitational accelerations measured by the accelerometer, respectively.

Fig. 8 shows the changes in the block conditions and sand surface level due to upward seepage flow for each case at 300 s (hydraulic gradient of approximately $i = 0.5$), 420 s (around the critical

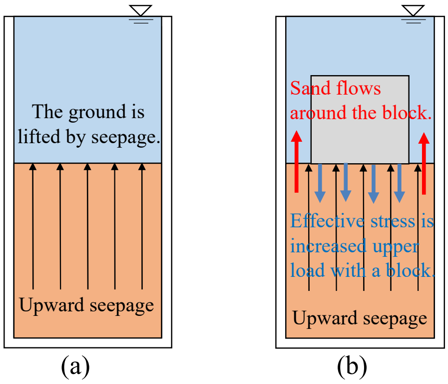

Fig. 9 The mechanism of block behavior subjected to seepage failure of ground: Case of ground only (a) and Case of a block placed on ground (b).

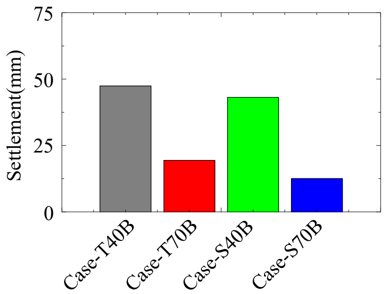

Fig. 10 Time histories of excess pore water pressure in case of soil ground only: Case-T40 (a); Case-T70 (b); Case-S40 (c) and Case-S70 (d)

hydraulic gradient, i_{cr}), and 1,200 s (at the end of the test). The hydraulic gradient in the ground increased as the hydraulic head difference increased in each case and reached the critical hydraulic gradient at a certain time (approximately 420 s). The critical hydraulic gradient is the same as the hydraulic gradient in the ground and does not consider the effect of overload due to the blocks. After the critical hydraulic gradient was reached, the hydraulic-head difference remained constant, but seepage failure did not occur, as in the soil-only case. This is because the ground resisted the seepage force because the blocks increased the effective stress owing to the overlying load. It is also possible that the area where the ground could flow away was limited between the block and the experimental apparatus; therefore, the ground resisted the flow to some extent. In the case of 40 % relative density using Toyoura sand (Case-T40), settlement began at a hydraulic gradient of i = 0.5, and the gradient of the settlement curve became steeper at the point where the maximum hydraulic head difference was reached (around 400 s), at which the gradient of settlement curve of the block was maximum. However, in other cases, the settlement tended to increase slowly. Moreover, in

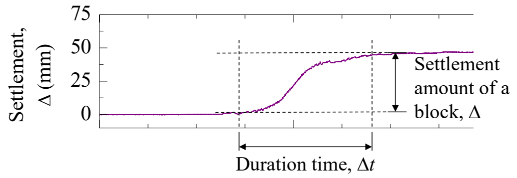

Fig. 11 Definition of the settlement rate of the block

Table 3 Settlement rate of a block in ground

Case	Settlement rate of a block (mm/s)
Case-T40B	0.134
Case-T70B	0.050
Case-S40B	0.049
Case-S70B	0.016

all cases, the settlement of the blocks ceased to a certain degree despite the continuous application of a seepage force equivalent to the critical hydraulic gradient. The tilt angle of the block from the time of its initial installation increased or decreased with settlement, suggesting that the block settled with rocking behavior starting around the y-axis. This change in tilt angle was observed at the same time as or even before the response of the block displacement meter and is considered to capture the fine behavior of the block.

5. DISCUSSIONS

5.1 Block Behavior Subjected to Seepage Failure of ground

Fig. 9 shows the behavior mechanism of the block subjected to ground penetration failure assumed from the results of this model test. For the one-dimensional seepage failure phenomenon, in the case of the ground only, the deformation of the soil was such that the entire ground was lifted by seepage flow. However, when a block was placed on the ground, the block weight acted as an overburden load on the ground and thus resisted seepage flow. Therefore, the ground flowed away from the left and right sides of the blocks, which were not subjected to overburden. The block then exhibited gradual settlement behavior, which was characterized by a hydraulic gradient of 0.5.

5.2 Settlement Phenomenon of Block

Fig. 10 shows the maximum settlement of the block in each cases. The settlement of the Block on Toyoura sand was slightly larger than that of the block on silica sand #8, regardless of the density; however, this difference was not significant. In the comparison by density of the ground, the settlement of the block in the loose ground with a relative density of 40% was approximately twofold that of the block in the medium dense ground with a relative density of 70% in this model test for both materials. It was again found that the denser the ground, the less likely it is to settle, although this depends on the boundary conditions and other factors.

5.3 Settlement Rate of Block

The settlement rate of the block was calculated from its settlement history using the method shown in Fig. 11 and is summarized in Table 3. Settlement rate was determined by dividing the amount of settlement of the block by the duration of settlement. The results showed that the settlement rate of the block on Toyoura sand was higher than that of the block on silica sand #8. At 40% relative density, the settlement rate of the block on the Toyoura sand was 2.7 times larger than that of the silica sand #8, and at 70% relative density, the settlement rate of the block on the Toyoura sand was 3.1 larger than that of the silica sand #8.

6. CONCLUSION

In this study, the seepage failure and block settlement phenomena were observed in detail and the following conclusions were reached:

- The critical hydraulic gradient at which the effective stress diminishes owing to the upward seepage force was dependent on the relative density of the soil ground, but independent of the type of geomaterial, with different grain size distributions. In the case of a seabed consisting of medium loose sand (D_r = 40 %), the concrete blocks started to sink at a hydraulic gradient of 90 % of the critical value. In the case of dense sand (D_r = 70 %), the concrete block sank near the critical hydraulic gradient.
- The concrete block resting on the soil ground of loose Toyoura sand sank quickly into the ground in a manner of progressive failure; in the other cases, the concrete block sank gradually. The settlement of the concrete block was capped at a certain level even when the hydraulic gradient reached a critical value.
- The monitoring of displacement and acceleration by using sensors installed on the blocks showed that the concrete blocks started to move around a hydraulic gradient of 50 % of the critical value, regardless of the geomaterial type and relative density.
- The tilting angle of the concrete block increased or decreased during the settlement progressed, indicating that the block settled with a rocking behavior around the horizontal axis.

7. ACKNOWLEDGMENTS

This work was supported by the JSPS Grant-in-Aid for Scientific Research (C) 17K06553 and JSPS Grant-in-Aid for Young Scientists 20K14824. The authors would like to thank Yudai Fuji for the help with the model tests.

8. REFERENCES

[1] Oka F., Yashima A., Miura S., Ohmaki S., and Kamata A., Settlement of breakwater on submarine soil due to wave-induced liquefaction, in Proc. 5th International Society of Offshore and Polar. Engineers, Vol. 1, 1995, pp. 237-242.

[2] Yamamoto T., Koning H. S. L., Sellmeijer H., and Van Hijum E., On the response of a pore-elastic bed to water waves, Journal of Fluid Mechanics, Vol. 87, No. 1, 1978, pp. 193-206.

[3] Miura K., Asahara S., Otsuka N., and Ueno K., Formulation of ground for coupled analysis of seabed response to wave loading, Proceedings of Geotechnical Engineering symposium, Vol. 49, 2004, pp. 233-240. (in Japanese)

[4] Zen K., and Yamazaki H., Mechanism of wave-induced liquefaction and densification in seabed, Soils and Foundations, Vol. 30, No. 4, 1990, pp. 90-104.

[5] Baldock T. E., and Holmes P., Seepage effects on sediment transport by wave and currents, Coastal Engineering, Vol. 1, No. 26, 1998, pp. 3601-3614.

[6] Matsuda T., Miura K., Takayanagi R., and Anai K., Wave flume experiment on wave response of a rectangle block under different seabed characteristics, Journal of Japan Society of Civil Engineers, Ser. B2 (Coastal Engineering), Vol. 75, No. 2, 2019, pp. 955-960. (in Japanese)

[7] Dean, R. G., Heuristic models of sand transport in the serf zone, Proc. Conf. Eng. Dyn. in Surf zone, 1973, pp. 208-214.

[8] Yoshimi Y., Kuwabara F., and Tokimatsu K., One-dimensional volume change characteristics of sands under very low confining stresses, Soils and Foundations, Vol. 15, No. 3, 1975, pp. 51-60.